We are IntechOpen, the world's leading publisher of Open Access books
Built by scientists, for scientists

4,800
Open access books available

122,000
International authors and editors

135M
Downloads

Our authors are among the

154
Countries delivered to

TOP 1%
most cited scientists

12.2%
Contributors from top 500 universities

CLARIVATE ANALYTICS
BOOK CITATION INDEX
INDEXED

WEB OF SCIENCE™

Selection of our books indexed in the Book Citation Index in Web of Science™ Core Collection (BKCI)

Interested in publishing with us?
Contact book.department@intechopen.com

Numbers displayed above are based on latest data collected.
For more information visit www.intechopen.com

Chapter 4

Dynamic Modeling of a Serial Link Robot Laminated with Plastic Film

Norimitsu Sakagami and Mizuho Shibata

Additional information is available at the end of the chapter

http://dx.doi.org/10.5772/intechopen.72441

Abstract

This chapter presents serial link robots laminated with a plastic film, a derivation of the equations of motion of the laminated robots, and numerical simulation. Recently, to become capable of wide application for several serial link robots that work outside, waterproofing and dustproofing techniques are required. We have proposed a robot packaging method to improve waterproof and dustproof properties of serial link robots. Using the proposed packaging method, rigid links with some active joints are loosely laminated with plastic film to protect the links from dust and water. In the next step of our research, we must derive the equations of motion of the laminated robots for the design and performance improvement from the viewpoint of high speed and high energy efficiency. We assume a plastic film as a closed-loop link structure with passive joints in this chapter. A rigid serial link (fin) connected with a motor-actuated joint moves a closed-loop link structure with passive joints. We numerically investigate the influence of the flexural rigidity of a plastic film on the motion of the rigid fin. This research not only contributes to the lamination techniques but also develops a novel application of waterproofing and dustproofing techniques in robotics.

Keywords: closed-loop mechanism, equations of motion, serial link robot, flexible mechanism, vacuum packaging, fish-like robots

1. Introduction

This chapter presents a description of equations of motion of serial link robots laminated with plastic film. Serial link robots are designed as a series of links connected by motor-actuated joints. Typical applications of serial link robots are serial manipulators, which are the most common industrial robots, such as pick-and-place assembly robots [1, 2] and welding robots [3, 4]. A salient feature of serial link robots is their large workspace in comparison with the robot size [5]. Additionally, serial link robots consist of simple structures. For that reason, they

INTECH
open science | open minds

© 2018 The Author(s). Licensee InTech. This chapter is distributed under the terms of the Creative Commons Attribution License (http://creativecommons.org/licenses/by/3.0), which permits unrestricted use, distribution, and reproduction in any medium, provided the original work is properly cited. CC BY

have also been used as various applications as humanoids [6, 7], robotic hands [8, 9], biped robots [10, 11], robotic legs [12, 13], snake robots [14, 15], fish-like robots [16, 17], and a jumping robot [18]. Kinematics of a serial link robot itself has remained a hot topic in robotics and has been studied for the last few decades [19].

Recently, to become capable of wide applications for several serial link robots that must be used outdoors, waterproofing and dustproofing techniques must be improved. These techniques have been developed for ocean engineering and field engineering for the past few decades. For example, most underwater robots have waterproof and pressure-tight housings made of metal such as stainless steel or titanium alloy [20–22]. In another waterproofing method used in ocean engineering, called the pressure equalization method, waterproof housings are filled with an insulating fluid such as an industrial oil or a cleaning fluid used for semiconductors. This method has been applied to underwater equipment of several types such as undersea batteries of a submarine [23] and light devices.

We have proposed a robot packaging method to improve waterproofing of a serial link robot [24]. In the robot packaging method, a serial link mechanism connected with motor-actuated joints is packaged in plastic film in a chamber of a vacuum packaging machine, so that the serial link robot is laminated with a plastic film (**Figure 1**). We applied the packaging method to fabrication of a fish-like robot (**Figure 2(a)**). The body (the float in **Figure 2(b)**) and fin (the oscillation plate in **Figure 2(b)**) are connected via a servo motor in series. The outer plastic film is inflected by the motion of the inside fin. The fish-like robot generates thrust using the body inflection underwater. This packaging method is applicable not only to a rotary joint

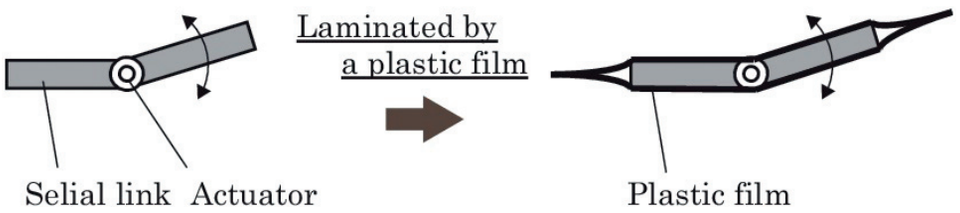

Figure 1. Concept of a serial link robot laminated with plastic film.

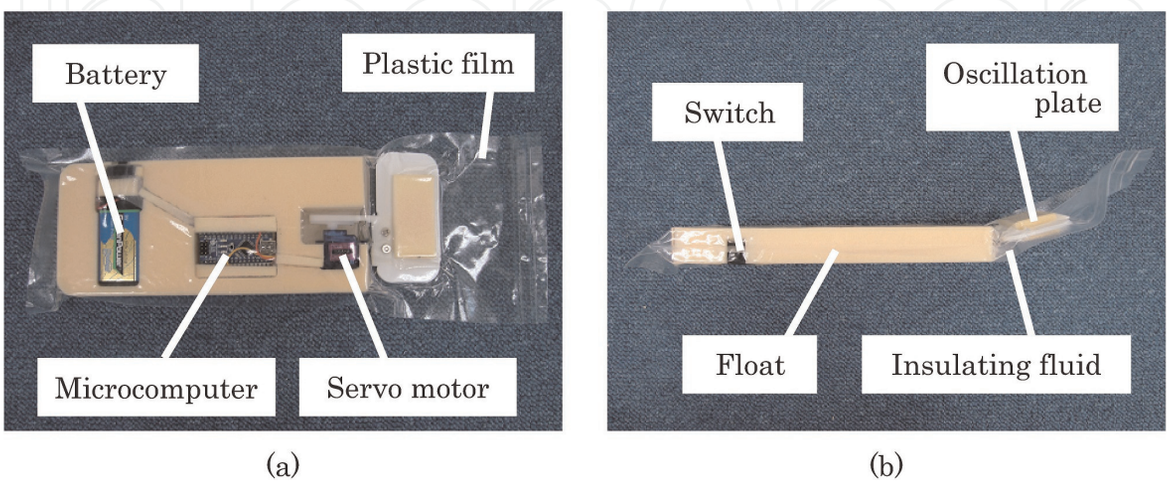

Figure 2. Concept of a fish-like robot laminated with plastic film.

mechanism but also to a prismatic joint mechanism. A ball-screw mechanism was packaged in plastic film to fabricate an attitude control system for underwater robots [25].

In the robot fabricated using the packaging method, the rigid links and the plastic film are loosely laminated. The serial link in the plastic film is packaged in the chamber of the vacuum packaging machine after the decompression process. No adhesion exists between the rigid link and the plastic film. However, the rigid link and the plastic film contact mutually with little slippage between them after depressurization during the robot packaging method. To move the serial link with an actuator in the plastic film, the actuator torque must overcome the static frictional force between the links and the film. We encapsulate an insulating fluid to improve lubricity between the links and the film. Therefore, we must consider not only the material properties of the plastic film but also the effects of the insulating fluid to improve the performance of the serial link robots.

In the next step of our research, we must derive equations of motion to achieve performance improvements such as thrust force and energy efficiencies of the laminated robot system. Over the past few decades, several researchers have studied models of laminated structures. In magnetics, modeling of hysteresis losses [26–28], eddy current losses [29, 30], and temperature effects [31] for magnetic laminations have been proposed under some conditions. Depending on those conditions, a 1-D model [32], a 2-D finite-element model [33], and a 3-D finite-element model [34] have been selected to analyze the laminated structure performance. However, we must derive the equations of motion and analyze the motions of laminated structures including a serial link robot from the viewpoint of robotics. In this chapter, we propose equations of motion of the laminated robot underwater. In addition, based on the equations of motion, we numerically estimate the influence of flexural rigidity of plastic films for the motion performance of the serial link robot.

This research not only contributes to lamination techniques but also develops a novel application of waterproofing and dustproofing techniques for application to robotics. Several techniques using an elastic material such as silicone have been applied to robots for waterproofing [35], impact absorption [36, 37], and decoration [38]. In terms of most of the robots that are covered with an elastic material, the actuator force and torque must overcome the elastic force during motions of the robot body. Thin plastic films can be flexible, but they have lower elasticity for bending than other elastic materials such as silicone. Therefore, we can select a low-force and torque actuator to inflect the robot body laminated with a thin plastic film.

This chapter is organized as follows: Section 2 briefly outlines the concept of a serial link robot laminated with a plastic film. This plastic film has flexible and nonextendable properties, which are useful for vacuum packaging in food industry. Also Section 2 takes applications of two serial link robots, such as fish-like robots we have proposed. Section 3 discusses derivation of the equations of motion of the serial link robots including a plastic film that laminates the robot body. Here, we assume that the plastic film has a closed-loop link structure with passive joints. A serial link as a fin connected by a motor-actuated joint drives the closed-loop link structure (the plastic fin) with passive joints. We consider equations of motion to estimate the motion characteristics of the proposed robot system. Section 4 presents validation of the equations of motion through several simulations. Section 5 presents a summary our future work and conclusions.

2. Application

In this section, we briefly describe the concept of lamination of a serial link robot for waterproofing and pressure tightness. In robotics, piezoelectric actuators have been used to drive several robots as a useful application of lamination techniques [39, 40]. We used a vacuum packaging machine to laminate a serial link robot with a plastic film. We designated this fabrication as "robot packaging."

2.1. Robot packaging method

Figure 3 presents the "robot packaging" process as an example of fabricating a fish-like robot. The entire robot body was covered by a flexible plastic film. The process is divisible into four steps: (a) encapsulation of the internal components, including a microcontroller, a drive circuit, a battery, a servomotor, and an oscillation plate, in a plastic film bag; (b) pouring of an insulating fluid, specifically industrial oil or cleaning fluid for semiconductors, into the plastic bag; (c) depressurization of the inside of the robot using a vacuum packaging machine. This process reduces the quantity of air in the film bag; and (d) sealing of the plastic film by a sealer within the chamber of the vacuum packaging machine after depressurizing.

This plastic film has flexible and nonextendable properties, which is used for vacuum packaging in food industry. This packaging method corresponds with the method used in the food industry [41]. The internal components including electrical circuits in the body of the robot are not shortened by the insulating fluid surrounding the circuits. Using this method, we can

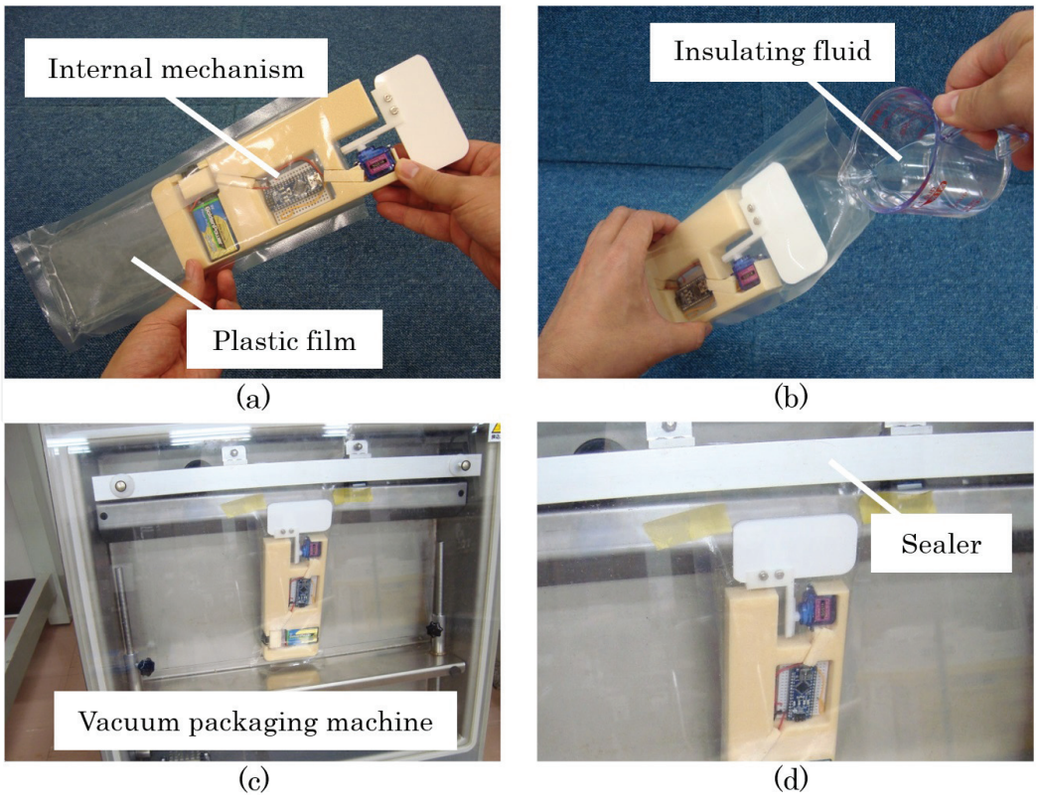

Figure 3. Fabrication process by robot packaging.

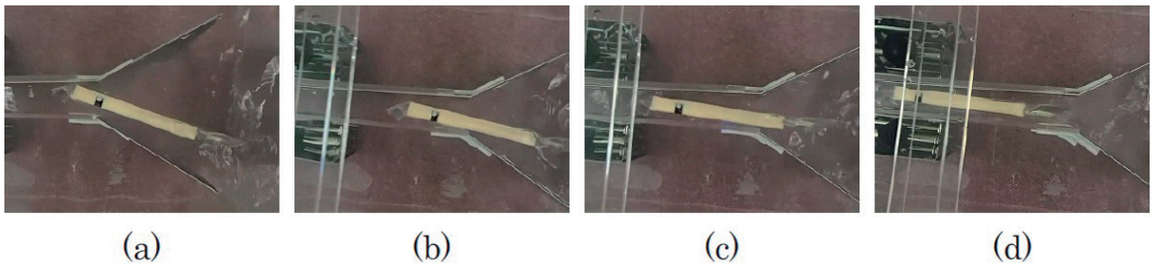

Figure 4. Swimming test of our prototype at narrow space.

readily fabricate the entire body of a serial link robot laminated with a plastic film at low cost and in a short time. The body can also be lighter than other underwater systems.

2.2. Fish-like robot laminated with a plastic film

As shown in **Figure 2**, we proposed a fish-like robot as a prototype hardware laminated using a plastic film, which was fabricated using a vacuum packaging machine. In the prototype robot, we applied an insulating fluid (Fluorinert FC-3283; 3 M Corp.) filled in the body. The insulating fluid is generally used as a cleaning fluid for semiconductors. The specific gravity of the insulating fluid is approximately 1.83, which is heavier than water. Therefore, we used a copolymer foam (NiGK Corp.) not only for the frame structure of the body but also for generating buoyancy. The specific gravity of the foam is approximately 0.2, which is a much lighter fluid than water.

We also applied a servomotor (SG51R; Tower Pro) to the prototype robot actuator. In this prototype, we used a microcontroller (Arduino Nano ver. 3.1). A styrene board of 80 mm height, 40 mm width, and 2 mm thickness was used as an oscillation plate to generate the thrust force of the prototype robot in water. The plastic film (poly bag TL12-38; Fukusuke Kogyo Co. Ltd.) covering the internal contents of the robot was multilayered for use in food packaging. This film is sealed by thermal adhesion of a vacuum packaging machine. We made use of a TM-HV made by Furukawa Mfg. Co., Ltd. as a vacuum packaging machine. In this prototype, the depressurization time is 15 s. The sealing time is 4.0 s. A battery (9 V) is used as the power source for driving the electrical circuits and servomotor.

After design, the prototype size without the film was approximately 185 mm long, 80 mm high, and 18 mm wide. After fabrication, the prototype including the film in **Figure 2** was 230 mm long, 90 mm high, and 18 mm wide. Additionally, it weighed approximately 290 g, including 80 ml of the insulating fluid, thereby realizing almost neutral buoyancy of the body. Under these conditions, the oscillation plate driven by the servo motor was moved 10 deg. in the left and right directions at a frequency of approximately 2.0 Hz (**Figure 4**).

3. Modeling

This section presents a discussion of the derivation of the equations of motion of a serial link robot laminated with a plastic film. The laminated robot consists of a rigid link fin, a plastic film, and an enclosed insulating fluid as illustrated in **Figure 5**. In this section, we assume that

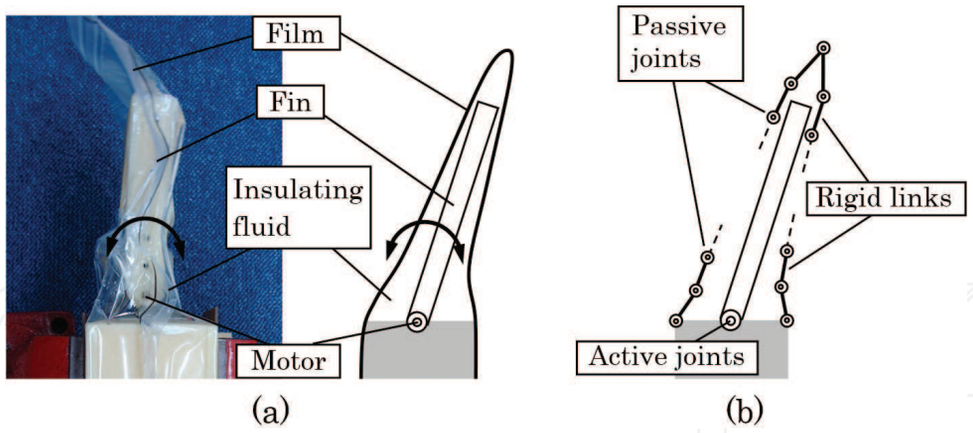

Figure 5. Modeling of a serial link robot laminated with a plastic film: (a) serial link robot laminated with a plastic film; (b) plastic film is modeled mathematically as a closed-loop link structure with multi-DOFs consisting of passive joints.

the plastic film is modeled as a multi-DOF closed-loop structure with passive joints that are actuated indirectly by a motor mounted on the base of the fin.

3.1. Rigid fin

The equation of fin motion in **Figure 5** is expressed simply as shown below.

$$I\ddot{\theta} = \tau \tag{1}$$

In this equation, scalar I represents the inertia of the rigid fin and the enclosed fluid, θ stands for the active joint angle of the fin, and the scalar τ includes an actuator torque and external torque related to the contact force from the film and additional inertia of the enclosed fluid.

To simplify the mathematical model of the contact force between the fin and the plastic film, we introduce a penalty method [42]. The penalty method treats elasticity and damping force for slight penetration between two objects. Here, we assume a small penetration between the fin and the joints of the links, as shown in **Figure 6(a)**. Contact force f_{pi} based on the penalty method is calculated as

$$f_{pi} = K_{pi}D_i - B_{pi}\dot{D}_i \tag{2}$$

where D_i denotes the small penetration between the fin and the plastic film at a contact point. K_{pi} and B_{pi} represent the elasticity and damping constant coefficients, respectively. As a result, the external torque τ_p generated by the contact forces f_{pi} can be calculated as

$$\tau_p = \sum_i \left(l_i \times f_{pi} \right) \tag{3}$$

where vector l_i represents the position for contact force f_{pi}.

In addition, the inertia of the enclosed fluid is included as well as the rigid inertia in the mathematical model because the rigid link fin carries the enclosed fluid during the fin motion.

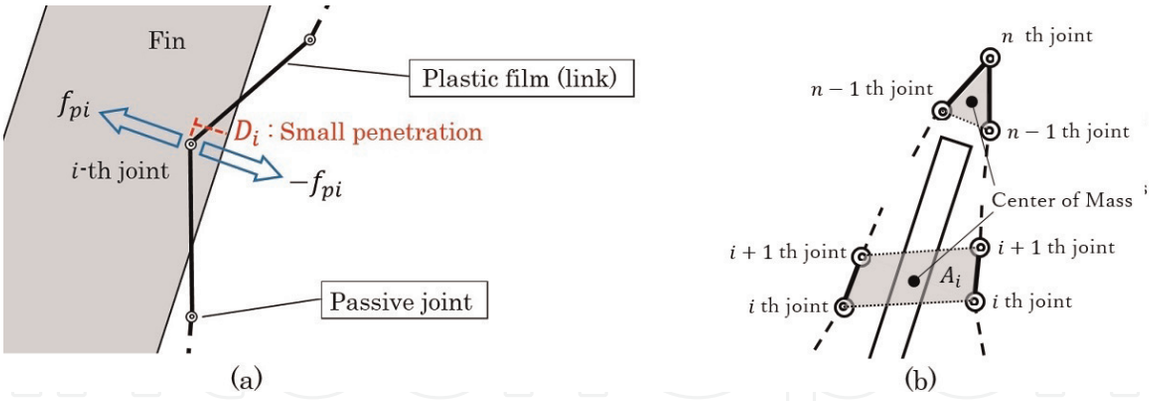

Figure 6. (a) Contact force between the fin and the plastic film based on the penalty method, and (b) calculation of the additional inertia of the enclosed fluid in the plastic film.

As illustrated in **Figure 6(b)**, a small area A_i of a trapezoid is determined by four points (or a triangle determined by three points at the tip of the fin,) and the center of the mass is used to estimate the fluid inertia. Mass M_{Fi} and inertia I_{Fi} of the fluid in a small area are obtained quantitatively as

$$M_{Fi} = A_i d\rho, I_{Fi} = M_{Fi} l_{Fi}^2 \tag{4}$$

where d, ρ, and l_{Fi} represent the depth of area A_i, the density of the insulating fluid, and the moment arm for the mass M_{Fi}, respectively. Consequently, the equations of the fin motion can be rewritten as follows.

$$(I_R + I_F)\ddot{\theta} = \tau_A + \tau_p \tag{5}$$

Therein, I_R signifies the inertia of the rigid fin. $I_F = \sum_j I_{Fi}$, τ_A stands for the actuator torque.

3.2. Plastic film

In this chapter, the plastic file is modeled as multi-DOF links with passive joints and with a closed kinematic loop constraint as illustrated in **Figure 7**. We use a method based on Lagrange-D'Alembert formulation on reduced system described in an earlier report [43, 44] to derive equations of motion of the closed-loop links.

First, a link of one of the closed-loop links, that is, is cut and a tree system (two serial link structures) is formed, as portrayed in **Figure 7**. Equations of motion of the serial link structures can be obtained easily using Newton-Euler method or Direct Lagrangian method. Because a plastic film is generally very light, the mass of the links can be negligible. Therefore, the equations of the motion of the multi-DOF serial link structures are only represented by passive joints with elasticity and damping effects:

$$B_R\dot{\theta}_R + K_R\Delta\theta_R = \tau_R \tag{6}$$

$$B_L\dot{\theta}_L + K_L\Delta\theta_L = \tau_L \tag{7}$$

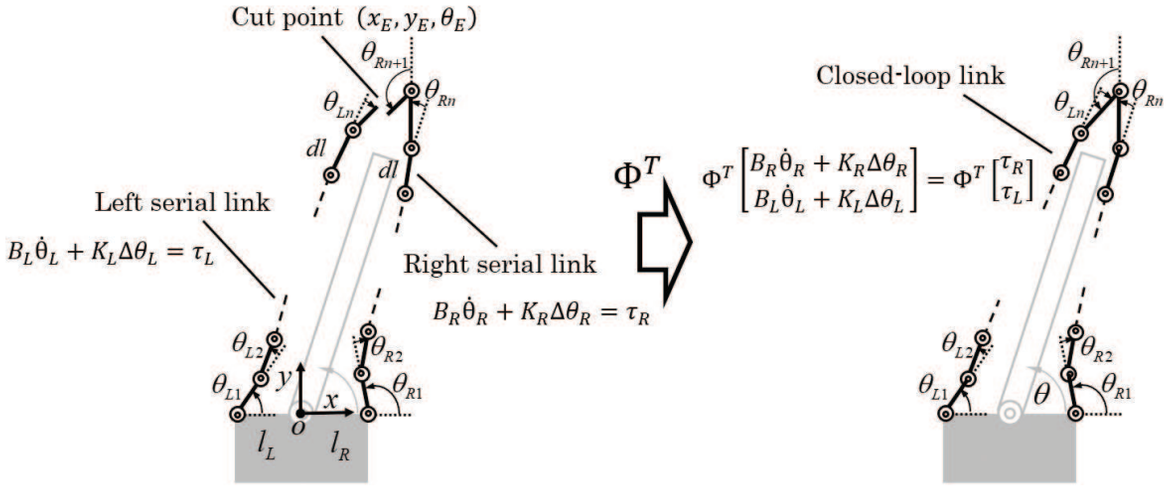

Figure 7. Mathematical model of the closed-loop link structure for a plastic film.

Therein, vectors $\theta_R = [\theta_{R1}, \cdots, \theta_{Rn+1}]^T$ and $\theta_L = [\theta_{L1}, \cdots, \theta_{Ln}]^T$ denote the passive joint angle vectors of the film, the vectors $\Delta\theta_R = \left[\tan\frac{\Delta\theta_{R1}}{2}, \cdots, \tan\frac{\Delta\theta_{Rn+1}}{2}\right]^T$ and $\Delta\theta_L = \left[\tan\frac{\Delta\theta_{L1}}{2}, \cdots, \tan\frac{\Delta\theta_{Ln}}{2}\right]^T$, where $\Delta\theta_{Ri}$ and $\Delta\theta_{Li}$ represent the rotational displacement for a joint. The matrices $B_R = \mathrm{diag}(b_{R1}, \cdots, b_{Rn+1})$ and $B_L = \mathrm{diag}(b_{L1}, \cdots, b_{Ln})$ represent the damping matrices, $K_R = \mathrm{diag}(k_{R1}, \cdots, k_{Rn+1})$ and $K_L = \mathrm{diag}(k_{L1}, \cdots, k_{Ln})$ are constant matrices related to the flexural rigidity and curvature of the plastic film. τ_R and τ_L represent the external torque related to the hydrodynamic effect acting on the film and the contact force between the rigid fin and the film, respectively.

Based on reports of the literature [43, 44], the equations of motion of the closed-loop structure is obtainable as

$$\Phi^T \begin{bmatrix} B_R\dot{\theta}_R + K_R\Delta\theta_R \\ B_L\dot{\theta}_L + K_L\Delta\theta_L \end{bmatrix} = \Phi^T \begin{bmatrix} \tau_R \\ \tau_L \end{bmatrix} \tag{8}$$

where Φ^T is the $(2n-2) \times (2n+1)$ matrix which comprises the Jacobian matrix of the constraint equations. Matrix Φ^T reduces the number of the equations from $(2n+1)$ to $(2n-2)$.

The following part of this discussion explains the external torque τ_R and τ_L. When forces f_i apply to their links, the torque is given as the following.

$$\begin{bmatrix} \tau_R \\ \tau_L \end{bmatrix} = \begin{bmatrix} \sum_i J_{Ri}^T(\theta_{Ri}) f_{Ri} \\ \sum_j J_{Lj}^T(\theta_{Lj}) f_{Lj} \end{bmatrix} \tag{9}$$

In that equation, J_{Ri} and J_{Li} are the Jacobian matrices of a contact point where a force is applied. Here, we consider forces related to the hydrodynamic effects and the contact forces between the plastic film and the rigid fin.

As described before, the contact force between the rigid fin and the film is derived based on the penalty method. The force applied to the film is expressed as

$$f'_{pi} = -f_{pi} = -\left(K_p D - B_p \dot{D}\right) \tag{10}$$

where f'_{pi} is the reaction force of f_{pi} in **Figure 6(a)**. Using Eq. (9), the torque related to the interference between the film and the fin is

$$\begin{bmatrix} \tau_{pR} \\ \tau_{pL} \end{bmatrix} = \begin{bmatrix} \sum_i J_{Ri}^T(\theta_{Ri}) f'_{piR} \\ \sum_j J_{Lj}^T(\theta_{Lj}) f'_{pjL} \end{bmatrix} \tag{11}$$

Finally, we assume that the hydrodynamic damping force acts as an external force on each link of the film. The hydrodynamic force acting on a link is modeled as shown below (**Figure 8**):

$$f_{Di} = \frac{1}{2} C_d \rho_w S_i |v_{\perp i}| v_{\perp i} \tag{12}$$

In this equation, C_d represents the drag force coefficient, ρ_w stands for the surrounding water density outside the film, S_i is the representative area of the ith link, and $v_{\perp i}$ is the relative flow velocity that is perpendicular to the ith link. We presume that the film moves in still water. The velocity of a link can be approximated by the following.

$$v_{\perp i} = R_i(\theta_i) J_i^T(\theta_i) \dot{\theta}_i \tag{13}$$

For vector $\theta_i = [\theta_{R1}, \cdots, \theta_{Ri}]^T$ or $\theta_i = [\theta_{L1}, \cdots, \theta_{Li}]^T$, matrix R_i is the rotational matrix to calculate the velocity perpendicular to the link. J_i is the Jacobian matrix of the *i*th link. However, we assume that $v_{\perp i} = 0$ $\left(f_{Di} = 0\right)$ when the *i*th link of the plastic film moves toward the rigid fin in the insulating fluid because the encapsulated insulating fluid in the plastic film moves with the fin and the film. Therefore, the relative velocity $v_{\perp i}$ between the film and the insulating fluid is almost zero.

Consequently, the external torque related to the contact forces and the hydrodynamic forces is summarized as shown below.

$$\begin{bmatrix} \tau_R \\ \tau_L \end{bmatrix} = \begin{bmatrix} \sum_i J_{Ri}^T(\theta_{Ri}) f'_{piR} + \sum_k J_{Rk}^T(\theta_{Rk}) f_{DkR} \\ \sum_j J_{Lj}^T(\theta_{Lj}) f'_{pjL} + \sum_k J_{Rk}^T(\theta_{Rk}) f_{DkR} \end{bmatrix} \tag{14}$$

In the model shown in **Figure 5**, three constraint equations related to the position $\left[x_E, y_E\right]^T$ and orientation θ_E of the two serial link structures should be considered. The constraint reduces the degrees of freedom of the serial link structures from $2n+1$ to $2n-2$. In other words, when configuration singularity does not occur, angular velocities $\left[\dot{\theta}_i, \dot{\theta}_j, \dot{\theta}_k\right]^T$ of any three joints of the closed-loop structure can be expressed by angular velocities of the $2n-2$ other joints.

$$\left[\dot{\theta}_i, \dot{\theta}_j, \dot{\theta}_k\right]^T = \mathrm{J}(\theta_R, \theta_L)\dot{q} \tag{15}$$

Therein, $\dot{q}$ is the $2n-2$ vector composed of all joint angular velocities except for $\dot{\theta}_i$, $\dot{\theta}_j$, $\dot{\theta}_k$ and $\mathrm{J}(\theta_R, \theta_L)$ is the $3 \times (2n-2)$ matrix derived from the constraint equations.

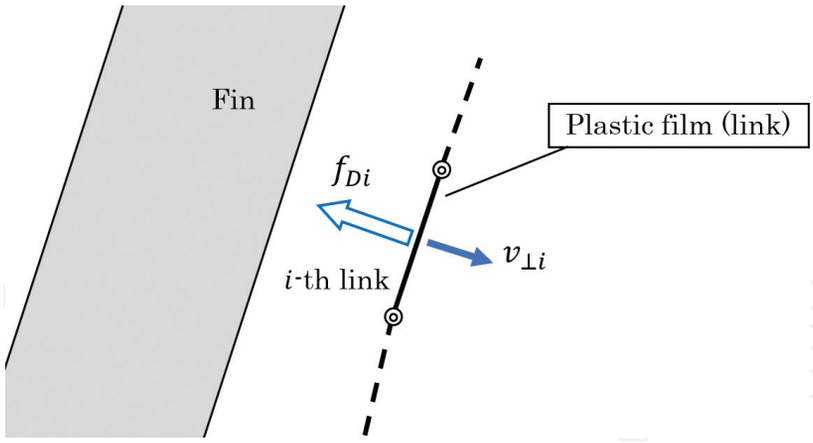

Figure 8. Model of the hydrodynamic damping force acting on the *i*th link.

Consequently, the equations of film motion are rewritten as shown below.

$$\left[\mathrm{B}' + J^T(\theta_R, \theta_L)\mathrm{B}''\mathrm{J}(\theta_R, \theta_L)\right]\dot{q} + \Phi^T \begin{bmatrix} K_R \Delta\theta_R \\ K_L \Delta\theta_L \end{bmatrix} = \Phi^T \begin{bmatrix} \tau_R \\ \tau_L \end{bmatrix} \tag{16}$$

Therein,

$$\mathrm{B}' = \begin{bmatrix} B'_R & 0 \\ 0 & B'_L \end{bmatrix}, \mathrm{B}'' = \mathrm{diag}\{b_i, b_j, b_k\} \tag{17}$$

where B'_R and B'_L denote the $(2n-2) \times (2n-2)$ matrices excluded the i, j, kth rows and columns from B_R and B_L, respectively . The characters b_i, b_j, b_k are the damping coefficients for the i, j, kth joints.

We use Eqs. (5) and (16) of the rigid fin and film motion for numerical simulation of the motion of the fin robot laminated by the plastic film.

4. Simulation

This section presents numerical simulation of the two-dimensional motion of the fin robot laminated by the plastic film. The purpose of the simulator is to design the laminated robots and to estimate their motion performance. A graphical simulator was developed for this purpose using software (Visual Studio 2010; Microsoft Corp.) and OpenGL library. The code was written in C language. The derived equations of the motion were solved numerically using the Runge-Kutta-Gill method by which the time step size was 0.001 s.

4.1. Numerical conditions

Table 1 presents the physical parameters of the laminated robot. We investigated the fin motion in three flexural rigidities of the plastic film. One was the value of the flexural rigidity of the film (3.14 gf cm^2) used to fabricate the fish robot (**Figure 2**). The other two values were 10

Moment of inertia of the fin [kg m^2]	I_R	0.0004033
b_{Ri} and b_{Li} in Eqs. (6) and (7)	b_{Ri}, b_{Li}	0.004
k_{Ri} and k_{Li} in Eqs. (6) and (7)	k_{Ri}, k_{Li}	0.001231
Position of the right 1st joint	$(l_R, 0)$	$(0.001, 0)$
Position of the left 1st joint	$(l_L, 0)$	$(-0.001, 0)$
Link length of the fin [m]	dl	0.005
Fin depth [m]	d	0.1
Density of insulating fluid [kg/m^3]	ρ	1830
Water density [kg/m^3]	ρ_W	1000
Representative area [m^2]	$S_i = d \times dl$	0.0005
Drag coefficient	C_D	1.3

Table 1. Parameters used for simulation.

times and 100 times the value of 3.14 (31.4 gf cm^2 and 314 gf cm^2). The plastic film had 41 passive joints to imitate a flexible film. The initial angles of the entire joints were set at 0 rad except for the following.

$$\theta_{R1} = \frac{92.86241\pi}{180}, \theta_{R17} = \frac{14.59520\pi}{180}, \theta_{R21} = \frac{145.08480\pi}{180}, \theta_{L1} = \frac{87.13760\pi}{180}, \theta_{L17} = -\frac{14.59520\pi}{180} \quad (18)$$

Based on the penalty method, the contact forces f_{pi} between the rigid fin and the entire joints of the plastic film were calculated using $f_{pi} = K_{pi}D_i - B_{pi}\dot{D}_i$ where $K_{pi} = 300$ and $B_{pi} = 0.1$ in the simulation.

The desired angle $\theta_d(t)$ [rad] for the rigid fin motion was given as

$$\theta_d(t) = \frac{\pi}{2} - \frac{\pi}{18}\sin(2\pi ft) \quad (19)$$

Frequency f of the fin motion was set at 2 Hz. For this desired angle, we made use of a conventional Proportional Derivative (PD) feedback controller $\tau_A = K_P[\theta_d(t) - \theta(t)] - K_D\dot{\theta}$ where $K_P = 30$ and $K_D = 0.1$. We assumed that a commercial waterproof servomotor (SG51R; Tower Pro) was used for the fin motion and assumed that the actuator had small lower and upper torque limits: $-0.0588 < \tau < 0.0588$ [Nm].

We presume that the relative flow velocity $v_{\perp i}$ for the calculation of the hydrodynamic force can be expressed approximately by the angular velocities $\dot{\theta}_R$ and $\dot{\theta}_L$ and joint angles θ_R and θ_L. There is no disturbance of water flow in the simulation.

4.2. Numerical results

We conducted a numerical simulation to investigate the fin motion of different flexural rigidities of the plastic film. **Figure 9** presents an illustration of how the fin changes in time series in the cases of (a) 3.14, (b) 31.4, and (c) 314 gf cm^2. **Figures 10** and **11** portray plots of the tracking

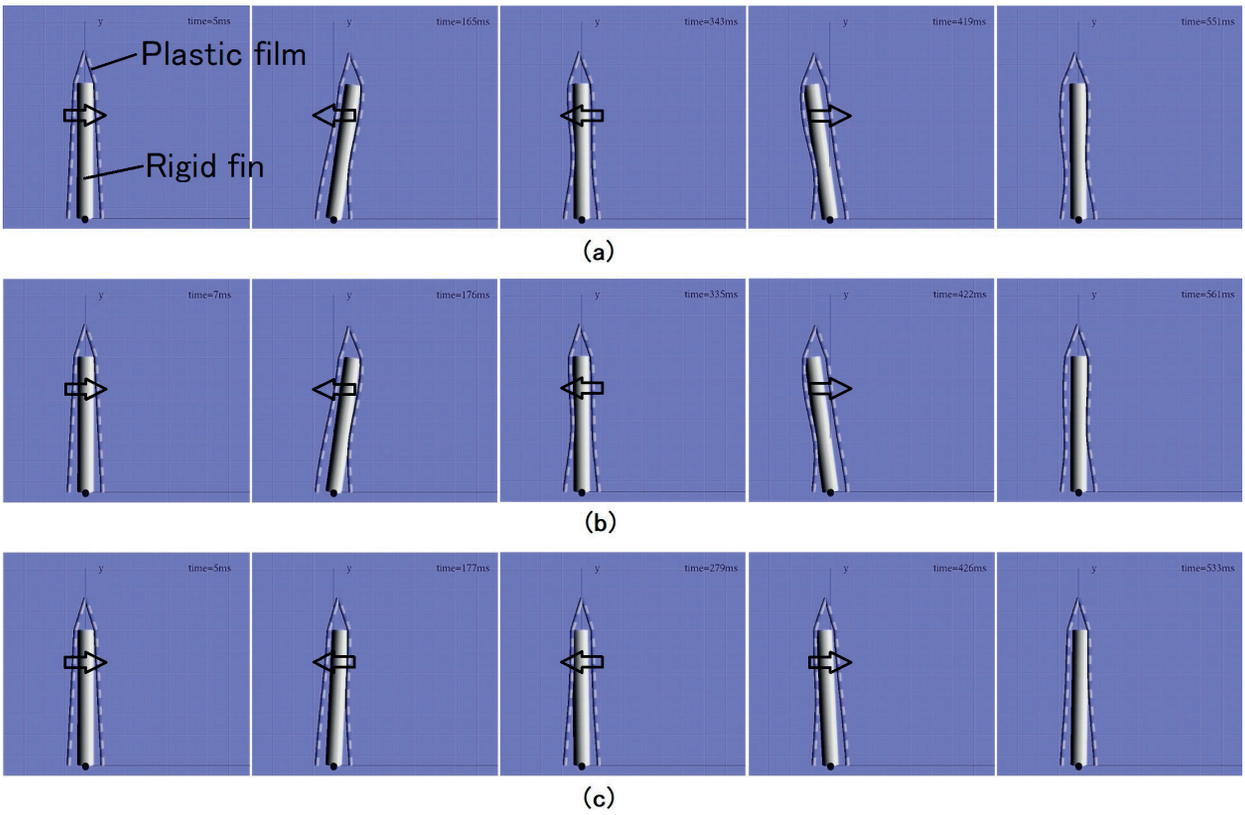

Figure 9. Two-dimensional simulation in three flexural rigidities of the plastic film. (a) 3.14, (b) 31.4, and (c) 314 gf cm^2.

data for the desired trajectory in Eq. (19) and the torque patterns in each case. For the value of 3.14 gf cm^2 in (a) that was the actual value for the prototype robot, the fin achieved smoothly reciprocating motion in the range of ± 8 degrees at 2 Hz in the simulation. The actual prototype robot in **Figure 4** also achieved approximately 10-deg. reciprocating motion at 2 Hz in the tank test. In (b), the flexural rigidity was 10 times different, no great difference in performance was found between the case (a) and the case (b). Result in (c) shows that higher flexural rigidity tended to prevent the fin motion. These numerical results demonstrate that the low torque actuator can inflect the robot body laminated by the thin plastic film with lower flexural rigidity.

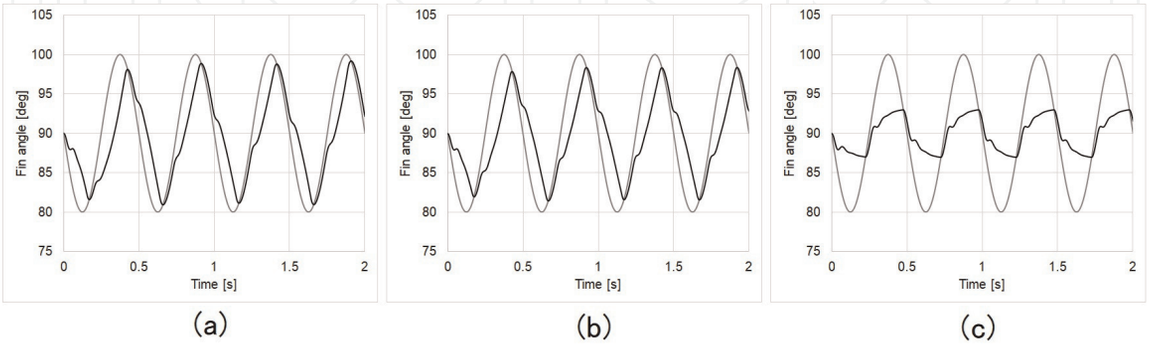

Figure 10. Tracking performance for the desired fin angle. (a) 3.14, (b) 31.4, and (c) 314 gf cm^2.

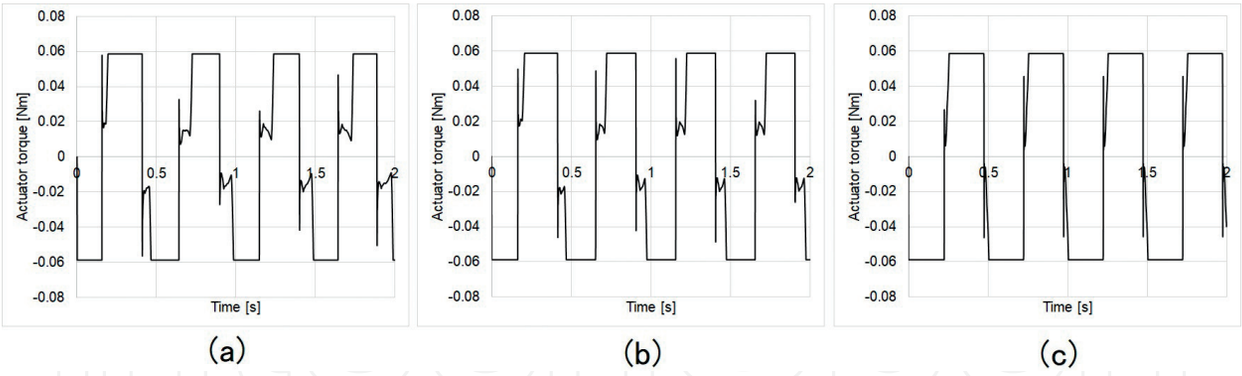

Figure 11. Torque pattern during the fin motion. (a) 3.14, (b) 31.4, and (c) 314 gf cm^2.

5. Conclusion

This chapter described the equations of motion of serial link robots laminated with a plastic film. We have proposed robot packaging method to improve waterproofing and dustproofing of serial link robots. To improve lubrication between the links and the film, we encapsulated an insulating fluid in the plastic film. Considering these conditions, we derived the equations of motion of the laminated robot to be useful for hardware design, motion analysis, and performance improvement such as thrust force and energy efficiency. In the derivation of the equations of motion, we assumed the plastic film as a closed-loop link structure with passive joints. Through numerical simulation based on the derived mathematical model of the fish-like robot, we estimated the motion performance of the fin in different flexural rigidities. We confirmed that the low torque actuator can inflect the laminated body because of the thin plastic film with lower flexural rigidity. Future work includes design of robots laminated with a plastic film using our mathematical model.

Acknowledgements

This work was partially supported by Furukawa Mfg. Co. Ltd. and partially by the Center of Innovation Program from Japan Science and Technology (JST) Agency. This work was also partially supported by JSPS KAKENHI (Grant Number 15 K18011).

Author details

Norimitsu Sakagami[1]* and Mizuho Shibata[2]

*Address all correspondence to: sakagami@scc.u-tokai.ac.jp

1 Department of Navigation and Ocean Engineering, School of Marine Science and Technology, Tokai University, Japan

2 Department of Robotics, Faculty of Engineering, Kindai University, Japan

References

[1] Lozano-Perez T, Jones JL, Mazer E, O'Donnell PA. Task-level planning of pick-and-place robot motions. Computer. 1989;**22**(3):21-29

[2] Wang D, Vidyasagar M. Modeling a class of multilink manipulators with the last link flexible. Transactions on Robotics and Automation. 1992;**8**(1):33-41

[3] Sicard P, Levine MD. An approach to an expert robot welding system. Transactions on Systems, Man, and Cybernetics. 1988;**18**(2):204-222

[4] Liu Y, Zhang Y. Toward welding robot with human knowledge: A remotely-controlled approach. Transactions on automation science and Engineering. 2015;**12**(2):769-774

[5] Siciliano B, Khatib O. Handbook of Robotics. 2nd ed. Spring; 2017

[6] Neo ES, Yokoi K, Kajita S, Kanehiro F, Tanie KA. Switching command-based whole-body operation method for humanoid robots. Transactions on Mechatronics. 2005;**10**(5):546-559

[7] Guan Y, Neo ES, Yokoi K, Tanie K. Stepping over obstacles with humanoid robots. Transactions on Robotics. 2006;**22**(5):958-973

[8] Bicchi A. Hands for dexterous manipulation and robust grasping: A difficult road toward simplicity. Transactions on Robotics and Automation. 2000;**16**(6):652-662

[9] Kawasaki H, Komatsu T, Uchiyama K. Dexterous anthropomorphic robot hand with distributed tactile sensor: Gifu hand II. Transactions on Mechatronics. 2002;**7**(3):296-303

[10] Huang Q, Yokoi K, Kajita S, Kaneko K, Arai H, Koyachi N, Tanie K. Planning walking patterns for a biped robot. Transactions on Robotics and Automation. 2001;**17**(3):280-289

[11] Grizzle JW, Abba G, Plestan F. Asymptotically stable walking for biped robots: Analysis via systems with impulse effects. Transactions on Automatic Control. 2001;**46**(1):51-64

[12] Ma S, Tomiyama T, Wada H. Omnidirectional static walking of a quadruped robot. Transactions on Robotics. 2005;**21**(2):152-161

[13] Hirose S, Fukuda Y, Yoneda K, Nagakubo A, Tsukagoshi H, Arikawa K, Endo G, Doi T, Hodoshima R. Quadruped walking robots at Tokyo Institute of Technology. Robotics & Automation Magazine. 2009;**16**(2):104-114

[14] Hirose S, Yamada H. Snake-like robots [Tutorial]. Robotics & Automation Magazine. 2009;**16**(1):88-98

[15] Tanaka M, Tanaka K. Shape control of a snake robot with joint limit and self-collision avoidance. Transactions on Control Systems Technology. 2017;**25**(4):1441-1448

[16] Conte J, Modarres-Sadeghi Y, Watts M, Hover FS, Triantafyllou MSA. Fast-starting mechanical fish that accelerates at 40 m/s2. Bioinspiration and Biomimetics. 2010;**5**(3):035004

[17] Yu J, Tan M, Wang L. Cooperative control of multiple biomimetic robotic fish. Recent Advances in Multi Robot Systems. 2008;**14**:263-290

[18] Higashimori M, Harada M, Ishii I, Kaneko M. Torque pattern generation towards the maximum jump height. In: Proceedings of IEEE International Conference on Robotics and Automation 2006. 1096-1101

[19] Craig JJ. Introduction to Robotics: Mechanics and Control. 3rd ed. Pearson.; 2004

[20] Eriksen CC, Osse TJ, Light RD, Wen T, Lehman TW, Sabin PL, Ballard JW, Chiodi AM. Seaglider: A long-range autonomous underwater vehicle for oceanographic research. Journal of Oceanic Engineering. 2001;**26**(4):424-436

[21] Sherman J, Davis RE, Owens WB, Valdes J. The autonomous underwater glider "spray". Journal of Oceanic Engineering. 2001;**26**(4):437-446

[22] Webb DC, Simonetti PJ, Jones CP. SLOCUM: An underwater glider propelled by environmental energy. Journal of Oceanic Engineering. 2001;**26**(4):447-452

[23] White DA. Modular design of Li-ion and Li-polymer batteries for undersea environments. Marine Technology Society Journal. 2009;**43**(5):115-122

[24] Shibata M, Sakagami N. Fabrication of a fish-like underwater robot with flexible plastic film body. Advanced Robotics. 2015;**29**(1):103-113

[25] Shibata M. Fish-like robot encapsulated by a plastic film. Recent Advances in Robotic Systems. Wang G editor. InTech. 2016:235-251. DOI: 10.5772/63506. Available from: https://www.intechopen.com/books/recent-advances-in-robotic-systems/fish-like-robot-encapsulated-by-a-plastic-film

[26] Zhang Y, Cheng MC, Pillay P. A novel hysteresis core loss model for magnetic laminations. Transactions on Energy Conversion. 2011;**26**(4):993-999

[27] Baghel APS, Chwastek K, Kulkarni SV. Modelling of minor hysteresis loops in rolling and transverse directions of grain-oriented laminations. Electric Power Applications. 2015;**9**(4):344-348

[28] Rasilo P, Singh D, Aydin U, Martin F, Kouhia R, Belahcen A, Arkkio A. Modeling of hysteresis losses in ferromagnetic laminations under mechanical stress. Transactions on Magnetics. 2016;**52**(3):7300204

[29] Khang HV, Arkkio A. Eddy-current loss modeling for a form-wound induction motor using circuit model. Transactions on Magnetics. 2012;**48**(2):1059-1062

[30] Hamzehbahmani H, Anderson P, Hall J, Fox D. Eddy current loss estimation of edge Burr-affected magnetic laminations based on equivalent electrical network part I: Fundamental concepts and FEM Modeling. Transactions on Power Delivery. 2014;**29**(2):642-650

[31] Chen J, Wang D, Cheng S, Wang Y, Zhu Y, Liu Q. Modeling of temperature effects on magnetic property of nonoriented silicon steel lamination. Transactions on Magnetics. 2015;**51**(11):2002804

[32] Petrun M, Steentjes S, Hameyer K, Dolinar D. 1-D lamination models for calculating the magnetization dynamics in non-oriented soft magnetic steel sheets. Transactions on Magnetics. 2016;**52**(3):7002904

[33] Jensen BB, Guest ED, Mecrow BC. Modeling overlapping laminations in magnetic core materials using 2-D finite-element analysis. Transactions on Magnetics. 2015;**51**(6):7403006

[34] Zheng W, Cheng Z. An inner-constrained separation technique for 3-D finite-element modeling of grain-oriented silicon steel laminations. Transactions on Magnetics. 2012;**48**(8): 2277-2283

[35] Sumoto H, Yamaguchi S. Development of a motion control system using phototaxis for a fish type robot In: Proceedings of the International Conference on Offshore and Polar Engineering 2010. pp. 307-310

[36] Kobayashi K, Yoshikai T, Inaba M. Development of humanoid with distributed soft flesh and shock-resistive joint mechanism for self-protective behaviors in impact from falling down In: Proceedings of International Conference on Robotics and Biomimetics 2011. pp. 2390-2396

[37] Hayashi M, Sagisaka T, Ishizaka Y, Yoshikai T, Inaba M. Development of functional whole-body flesh with distributed three-axis force sensors to enable close interaction by humanoids. In: Proceedings of International Conference on Intelligent Robots and Systems 2007. pp. 3610-3615

[38] Aono T, Nakamura Y. Design of humanoid with insert-molded cover towards the variety of exterior design of robots. In: Proceedings of International Conference on Intelligent Robots and Systems 2005. pp. 3342-3347

[39] Erturk A. Macro-fiber composite actuated piezoelectric robotic fish. In: Robot Fish: Bio-inspired Fishlike Underwater Robots 2015. pp. 255-283

[40] Shintake J, Shea H, Floreano D. Biomimetic underwater robots based on dielectric elastomer actuators. In: Proceedings of International Conference on Intelligent Robots and Systems 2016. 4957-4962

[41] Ahvenainen R. Novel Food Packaging Techniques. Woodhead Publishing.; 2003

[42] Tamamoto T, Koganezawa K. Multi-joint gripper with stiffness adjuster. In: Proceedings of 2013 IEEE/RSJ International Conference on Intelligent Robots and Systems (IROS). 2013. pp. 5481-5486

[43] Yiu YK, Cheng H, Xiong ZH, Liu GF, Li ZX. On the dynamics of parallel manipulators. In: Proceedings of the IEEE International Conference on Robotics and Automation. 2001. pp. 3766-3771

[44] Sakagami N, Otomasu K, Choi SK. Modeling and simulation of closed-loop mechanical systems for underwater applications. In: Proceedings of the 47th ISCIE International Symposium on Stochastic Systems Theory and Its Applications. 2015. pp. 247-252